

Adsorption of a carbon atom on the Ni₃₈ magic cluster and three low-index nickel surfaces: A comparative first-principles study

Q.-M. Zhang,¹ Jack C. Wells,² X. G. Gong,³ and Zhenyu Zhang^{4,5}¹*Department of Physics, University of Texas at Arlington, Texas 76019-0059, USA*²*Center for Engineering Science Advanced Research, Computer Science and Mathematics Division, Oak Ridge National Laboratory, Oak Ridge, Tennessee 37831-6355, USA*³*Department of Physics, Fudan University, 200433-Shanghai, People's Republic of China and Institute of Solid State Physics, Academia Sinica, 230031-Hefei, People's Republic of China*⁴*Condensed Matter Sciences Division, Oak Ridge National Laboratory, Oak Ridge, Tennessee 37831-6032, USA*⁵*Department of Physics, University of Tennessee, Knoxville, Tennessee 37996, USA*

(Received 5 September 2003; revised manuscript received 14 January 2004; published 28 May 2004)

Significant current interest exists in the catalytic growth of carbon (C) nanotubes on clusters of transition metal catalysts. Here we focus on the elemental energetics for the atomistic rate processes involved in the initial stages of the growth by studying a C atom on a nickel (Ni) magic cluster (Ni₃₈), which preserves fcc geometry, and three low-index extended Ni surfaces. Our methods are based on density-functional theory. The binding energies of a C atom on the extended Ni surfaces and the corresponding facets on the Ni cluster have been obtained and compared. In spite of the large difference in the curvature, the preference order of the adsorption sites for both the cluster and the extended surfaces is unchanged, which shows that among the stable (100), (111) hcp, and (111) fcc sites the (100) has the lowest energy. The diffusion barriers for a C atom on the three low-index surfaces, namely (100), (110), and (111), have also been obtained, with the highest mobility on the Ni(111) surface.

DOI: 10.1103/PhysRevB.69.205413

PACS number(s): 68.43.Fg, 61.46.+w, 68.43.Bc, 68.43.Jk

I. INTRODUCTION

It has been known for a long time that transition metals such as Fe, Co, and Ni are catalytic particles for the growth of carbon filaments.¹ The same essential role has been shown recently in the growth of the single-wall carbon nanotubes (SWNTs), which has drawn intense interest from the scientific community due to the outstanding properties of SWNTs and their potential applications. SWNTs can presently be produced by many methods, such as electric arc-discharge,² laser ablation of carbon,^{3,4} solar energy method,⁵ and catalytic methods.⁶⁻⁸ The catalytic methods are medium temperature synthesis techniques where the carbon source is obtained from the decomposition of carbon-containing gas molecules. Regardless of which synthesis technique is used, however, an important common feature of these methods is that small clusters of certain transition metals (Fe, Co, and Ni) and rare earth metals (Y and La) or their mixtures are used and found to be essential in high-yield SWNTs formation. The morphologies of grown SWNTs are observed to be directly related to the particle size.

In spite of intensive experimental and theoretical studies in the field, the fundamentals of these catalytic growth processes remain unclear. Questions to be answered include why the clusters rather than one of the extended surfaces are effective catalysts. One obvious difference between a cluster and an extended surface is that a cluster has a variety of facets. The facets may play complementary roles in the catalysis process: one could control feedstock decomposition, while others may serve to promote nucleation. To understand these fundamentals, it is worthwhile to determine the preferred adsorption sites and relative mobility of carbon on

various low-index surfaces. Such information is difficult to obtain from experiment, but may be obtained from theoretical analysis.

In the present work, we choose nickel (Ni) as a prototype element for these catalytic materials and study the elemental processes involved in the very initial stages of the nucleation of carbon (C) on its surfaces by first-principles methods. The typical sizes of the catalytic particles observed in many growth experiments range from a few nm to much larger systems that are currently not feasible for a first-principles calculation. Hence we approach the subject under investigation by consideration of two extreme cases: a small cluster containing 38 Ni atoms (Ni₃₈), and several extended low-index Ni surfaces. Even with this cluster's small size, it preserves many crystalline features. The magic Ni₃₈ cluster keeps the highly symmetric bulk fcc arrangement for Ni atoms and has six (100) minifacets and eight (111) minifacets, as shown in Fig. 1. The extended surfaces can be thought of as a cluster surface in the macroscopic limit. We focus on the

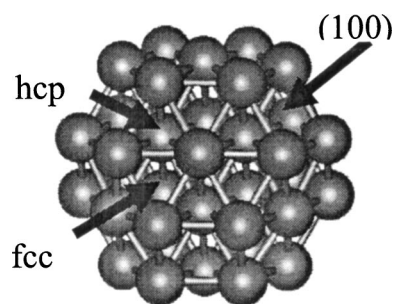


FIG. 1. The high-symmetric Ni₃₈ cluster has an fcc structure. The three stable adsorption sites are indicated.

TABLE I. The summary of published results from model calculations of surface binding energies (E_b), bond lengths (R_{C-Ni}), and the comparison with experimental values for carbon adsorption on Ni surfaces.

	Ni surface	BEBO (Ref. 12)	EMT (Ref. 17)	PCV (Ref. 19)	ASED-MO (Refs. 20 and 21)	MP (Ref. 22)	Experiment
E_b (eV)	(100)	7.43	6.5 8.10			7.69	7.35 ^{11,12} 7.37 ⁹ 7.55 ¹³
	(110)	3.93				6.47	
	(111)fcc	6.63	6.4 8.25	6.47	3.82 ²⁰ 8.59 ²¹	6.23	< 6.94 ¹² 6.9 ^{14,a}
	(111)hcp	5.33		6.47	3.94 ²⁰ 8.74 ²¹	6.24	< 6.94 ¹² 6.9 ^{14,a}
R_{C-Ni} (Å)	(100)		1.91 1.85			1.77	1.80 ± 0.015 ²³ 1.82 ± 0.05 ²⁴ 1.89 ± 0.05 ²⁵ 1.85 ± 0.06 ²⁶ 1.79 ± 0.03 ²⁷
	(110)					1.80	
	(111)fcc		1.83 1.77		2.00 ²⁰ 2.01 ²¹	1.85	1.90 ^{28,b}
	(111)hcp				1.97 ²⁰ 2.01 ²¹	1.84	

^aExperimental result obtained for polycrystalline aluminum-supported nickel catalysts.

^bExperimental result obtained for graphitic carbon on the Ni(111) surface.

adsorption and diffusion of one C atom on the surfaces of these systems and want to understand the comparison between these two limiting cases. Our results show that the Ni(100) surface is favored for C adsorption among the low index surfaces while the Ni(111) surface has the highest mobility for a C atom. Despite the huge difference in the curvature for the Ni₃₈ cluster and the extended surfaces, the preference sequence of the adsorption sites is the same.

II. PREVIOUS WORK

The majority of previous investigations aimed at understanding the interaction of carbon with transition metal surfaces have been motivated by the need to understand catalytic hydrocarbon synthesis.⁹ However, experimental data for the fundamental thermodynamic quantities, such as the bonding energy of atomic carbon on single crystal surfaces, are scarce. The only known data for single crystal surfaces exists in a series of articles by Blakely and co-workers,¹⁰⁻¹³ in which the binding energy for carbon was estimated through a thermodynamic cycle using the measured heats of segregation, vaporization, and solution. Their measured binding energies are 7.35 eV for Ni(100) and an upper limit of < 6.94 eV for Ni(111). The thermodynamic properties of surface carbon on polycrystalline nickel surfaces have been studied by observing the Boudouard equilibrium, $2CO \leftrightarrow C + CO_2$,¹⁴ and are qualitatively consistent with results from surface segregation on single-crystals surfaces (e.g., the C binding energy was measured as 6.9 eV). Recently, the binding energies of C to Ni_n cluster cations has been measured for $2 \leq n \leq 16$ (Ref. 15) using guided ion beam techniques similar to those used for C binding to Fe_n cluster cations.¹⁶

The binding energy as a function of cluster size varies strongly for $n < 5$, and largely saturates for $n \geq 5$ to values very close to C binding to bulk Ni surfaces.¹⁵

Theoretical model studies have been performed to interpret experimental results and to fill voids in available data on carbon adsorption to Ni surfaces. Blakely and co-workers provided estimates of C bonding to Ni surfaces, using the bond-order/bond-energy (BOBE) method, which are quite accurate compared to their measurements [7.43 eV for Ni(100), 6.63 eV for the fcc surface of Ni(111)]. The BOBE method is motivated by the understanding that the Ni-C interaction is primarily local in character.¹² Varying combinations of effective-medium theory (EMT) and quantum-mechanical calculations have been used in reaching contrasting carbon chemisorption pictures.^{17,18} The model of polar covalence developed by Sanderson was used to calculate binding energies of 6.47 eV at zero coverage for C adsorbed at the fcc hollow site and hcp hollow site on the Ni(111) surface.¹⁹ The atom superposition and electron delocalization molecular orbital (ASED-MO) method has been applied to estimate surface adsorption.^{20,21} A Morse potential (MP) parameterization of the Ni-C interaction²² has been applied to predict a variety of thermodynamic quantities. For C binding energies on Ni surfaces, the MP method predicts 7.69 eV for the (100), 6.47 eV for the (110), and 6.23 and 6.24 eV for the fcc and hcp sites on the (111) surface. (See Table I for a summary of published results from model calculations of surface binding energies and comparison with experimental values.)

In addition to the inherent interest resulting from their primary role in catalysis, description of atomic adsorption on

TABLE II. The present work and the summary of published *ab initio* theoretical values obtained using cluster and periodic surface models along with a comparison with experiment for carbon adsorption on Ni surfaces. The Ni₃₈ cluster in the present work has a full relaxation, while in the previous calculations using cluster models (columns 3–5), the geometry of the Ni cluster is fixed to mimic the Ni(100) surface.

	Ni surface	DFT-LDA Ni ₉	DFT-GGA Ni ₁₃	CASSCF Ni ₅	Present work: Ni ₃₈	DFT-GGA surface	Present work: surface	Experiment
E_b (eV)	(100)	11.4 ³¹ 11.8 ^{33,c} 11.5 ^{33,d}	6.17 ³⁴	6.50 ³²	8.26		8.43	7.35 ^{11,12} 7.37 ⁹ 7.55 ¹³
	(110)						7.65	
	(111)fcc				7.14	6.68 ³⁹ 6.35 ⁴⁰	7.18	< 6.94 ¹² 6.9 ^{14,a}
	(111)hcp				7.29	5.97 ³⁹	7.25	< 6.94 ¹² 6.9 ^{14,a}
R_{C-Ni} (Å)	(100)				1.83		1.85	1.80 ± 0.015 ²³ 1.82 ± 0.05 ²⁴ 1.89 ± 0.05 ²⁵ 1.85 ± 0.06 ²⁶ 1.79 ± 0.03 ²⁷
	(110)						1.90	
	(111)fcc				1.77	1.79 ³⁹ 1.76 ⁴⁰	1.77	1.90 ^{28,b}
	(111)hcp				1.76	1.89 ³⁹	1.77	

^aExperimental result obtained for polycrystalline aluminum-supported nickel catalysts.

^bExperimental result obtained for graphitic carbon on the Ni(111) surface.

^cLocal spin-density (LSD) calculation, no spin polarization (singlet).

^dLocal spin-density (LSD) calculation, spin polarization (triplet).

transition metal surfaces provides discriminating insight into the electronic structure of transition metal systems, whose *ab initio* description is well-known to be a challenging task due to the presence of unfilled *d*-electron shells.^{29,30} In an effort to reduce the computational demand imposed by more rigorous calculations of chemisorption energies on surfaces, early *ab initio* calculations employed cluster models of various sizes and shapes.^{31–34} Typically, in these calculations, the geometry of the Ni cluster is arranged according to the geometry of a low-index Ni surface, and not relaxed to the ground-state configuration of a particular cluster. References 31 and 33 computed binding energies for a carbon atom on a Ni₉ cluster as a model for the (100) surface of Ni using density-functional theory (DFT) in the local-density (LDA) and local-spin-density (LSD) approximations. While providing valuable structural information, these calculations overpredict the absorption energy as 11.4 and 11.5 eV, respectively. This behavior is consistent with the well-established trend of LDA calculations to overpredict binding energies.^{35–38} The generalized gradient approximation (GGA) for the exchange-correlation energy functional was designed, in part, to correct the systematic overbinding of LDA calculations. Reference 34 used the DFT-GGA method to predict the binding energy of C on the (111) surface of Ni, using Ni₇ and Ni₁₃ cluster models, as 5.79 and 6.17 eV, respectively. Using the complete-active space, self-consistent field (CASSCF) method, Ref. 32 predicted the C binding

energy on the (100) surface of Ni to be 6.50 eV using a Ni₅ cluster model.

Reference 39 improved the quantitative, *ab initio* theoretical description of C adsorption on Ni(111) single crystal surfaces by performing calculations with periodic surface models, allowing the surface coverage dependence to be studied and finite cluster-size effects to be eliminated. This work used the DFT-GGA and the full-potential linear augmented plane wave (FP-LAPW) method to compute C binding energies on the Ni(111) surface of 6.68 eV for fcc sites and 5.97 eV for hcp sites, and recognized the preference for high coordination sites in C adsorption on Ni surfaces. Reference 40 reports binding energies for C on a periodic Ni(111) surface to be 6.35 eV, using a plane wave, pseudo-potential DFT-GGA method very similar to that used in our present work and described immediately below. (See Table II for a summary of published *ab initio* theoretical values obtained using cluster and periodic surface models, together with the present work, along with a comparison with experiment for carbon adsorption on Ni surfaces.)

III. METHODS

Our work is based on density functional theory using the generalized gradient approximation (GGA) for the exchange-correlation functional. The Vienna *ab initio* simulation package (VASP)⁴¹ is used in the calculations. For the GGA exchange-correlation functional, we use the PW91⁴² scheme,

which gives satisfactory results in many studies of strong adsorptions on metal surfaces.⁴³ We describe the interaction from core electrons through ultrasoft pseudopotentials^{44,45} for both Ni and C, and expand one-electron Kohn-Sham states in a plane wave basis with kinetic energies up to a cutoff of 21 Ry. We use supercell geometry with periodic boundary conditions for all surface and cluster systems considered. All calculations were performed non-spin-polarized, which reduced the total computational effort by a factor of 2. Since nickel is a weak magnetic material, a spin-polarized calculation on binding energies may cause a difference about 0.1 eV, as discussed in Ref. 50 for H adsorption on Ni surfaces, and Ref. 39 for C adsorption on the Ni(111) surface. But it should not change the geometries or the relative ordering of the binding energies. For small Ni clusters, it should also be weakly magnetic at zero temperature according to the trend in the work published by Reddy *et al.*⁴⁶

As a test of the accuracy of our approach, the dimmers of Ni₂ and C₂ have been computed. Our calculated bond lengths are 2.104 and 1.269 Å for Ni₂ and C₂, respectively, which are reasonably good comparing with corresponding 2.155 and 1.243 Å from experiments.^{47,48} The binding energies are 2.78 eV for Ni₂ and 6.52 eV for C₂,⁴⁹ comparing to 2.07 and 6.20 eV for the two dimers from experiments,⁴⁷ respectively. A test at a higher energy cutoff (25 Ry) for plane wave basis resulted in a change of 0.2% or less.

For all Ni₃₈ calculations, an fcc supercell with the cubic side length of 24 Å is used. That gives a nearest-neighbor distance of about 17 Å, leaving a surface at least 9 Å away from the surface of a neighboring cluster. To model the three low-index Ni extended surfaces, a slab with periodic boundary conditions in a supercell is used. For the (100) surface, a two-layer (6×6) unit cell slab is used, totaling 72 Ni atoms in a tetragonal supercell. For the (111) surface, a two-layer (6×6) unit cell slab is chosen in a hexagonal supercell. For the not so close-packed (110) surface, a three-layer (6×4) unit cell slab is used in an orthorhombic supercell with the two edges of the supercell of more or less the same size. The vacuum separating the slabs due to the periodic boundary condition in the direction normal to the surfaces is at least 12 Å wide. There are 72 Ni atoms in each slab. Since the adsorption energy, which is in opposite sign of the binding energy, of a C atom on each surface is the difference in energy between the adsorbed slab and the sum of the same clean slab and an isolated C atom, the influence due to the slightly different supercells used should be negligible here. In geometry optimizations, the top layer of the (100) and (111) surfaces and the top two layers of the (110) surface plus the adsorbed C atom, which is on the top layer only, are fully relaxed while the atoms in the bottom layer of a slab are fixed at their respective bulk positions. Considering the large size of the supercells chosen, only the Γ point is used for the Brillouin zone sampling. We have tested this choice by using a 2 special k -points sampling calculation for a randomly picked (100) supercell, the adsorption energy difference against the Γ point sampling is only ~ 0.03 eV, which is sufficient for the energies discussed in this work. To check the thickness convergence of the slabs chosen above, the thicknesses of the slabs were doubled while the smaller lat-

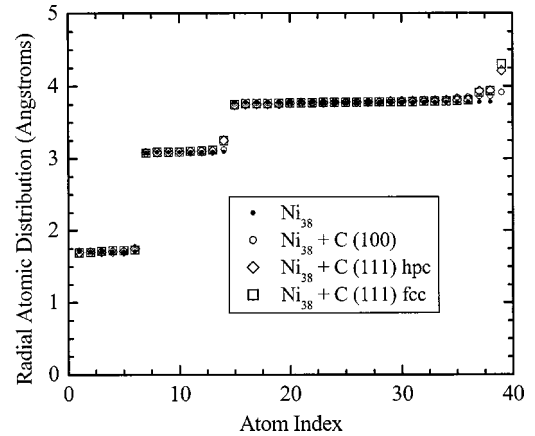


FIG. 2. The radial distances of the atoms for the four cases of a Ni₃₈ cluster, i.e., a pure cluster, and a C atom adsorbed on the three stable adsorption sites. For the adsorption cases, the 39th (the last) atom is the C atom.

eral dimensions were used with 4 special k -points sampling. The binding energies of C on (100) and (110) surfaces were increased by less than 1%, while that on (111) sites were lowered by $\sim 1\%$ and $\sim 2.5\%$ for fcc and hcp, respectively. These tests justified our choice of the slabs.

IV. RESULTS AND DISCUSSION

The Ni₃₈ cluster represents a magic number in the simulated annealing studies on the structures of Ni_{*n*} ($n = 2 - 55$),⁵² where a peak occurs in the energy difference $E(n-1) - E(n)$ at $n = 38$. The ground state structure obtained from Ref. 52, which was in agreement with the recent experiment,⁵³ has been completely relaxed in our first-principles calculation. The obtained structure preserves the high symmetry, having a truncated octahedron, or fcc geometry, as shown in Fig. 1. A radial distribution analysis shows that the Ni atoms are divided into three layers from the center of the cluster (see Fig. 2). At this size, 32 out of 38 atoms of the cluster are surface atoms. They form two sets, 24 identical atoms that arise from the edges of all the facets and eight identical atoms at the center of each of the eight (111) facets.

When a C atom is adsorbed on the cluster surface, three stable adsorption sites are found. One is the hollow site on the (100) facet, with a coordination of four Ni atoms. The other two are fcc and hcp sites on the (111) facet, with a coordination of three Ni atoms. The cluster experiences only minor relaxations after the C atom adsorptions, which are clearly shown in Fig. 2. The binding energies for the three sites are calculated from the total energy of the C adsorbed cluster with respect to those of Ni₃₈ and a single C atom [Reference state 3P (Ref. 49)], i.e., $E_b = E_{\text{tot}}(\text{Ni}_{38}) + E_{\text{tot}}(\text{C atom}) - E_{\text{tot}}(\text{C/Ni}_{38})$. They are listed in Table II, together with the corresponding nearest-neighbor C-Ni bond lengths. The (100) site has the highest binding energy for the adsorbed C atom, 8.26 eV. The binding energies for hcp and fcc sites of the (111) facet are 0.97 and 1.12 eV lower, respectively. This is due to the higher coordination number of

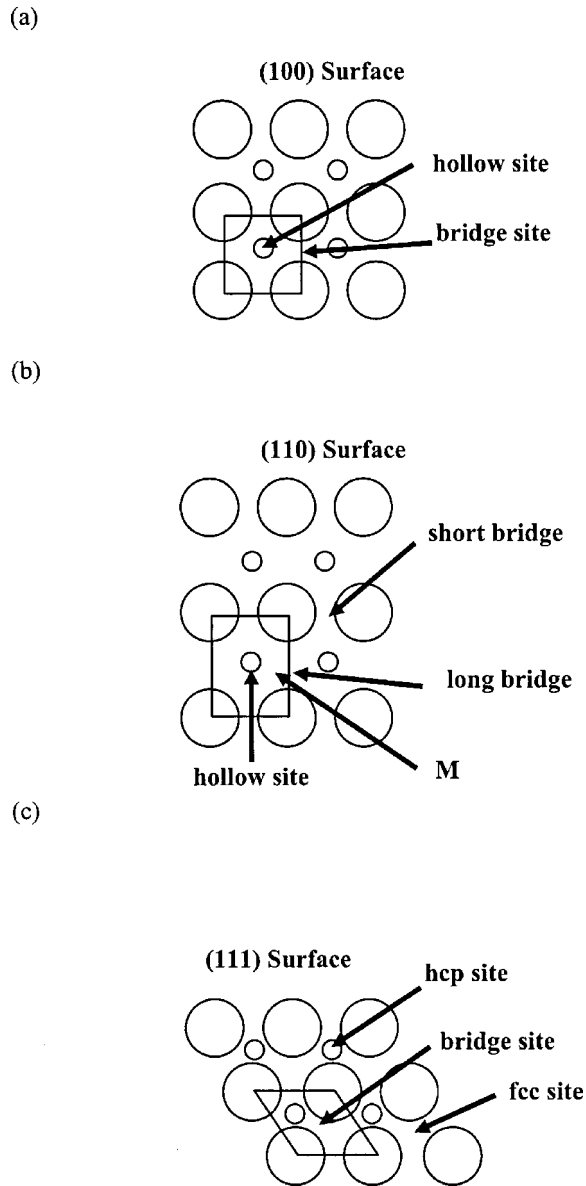


FIG. 3. The schematic top views of the extended Ni surfaces: (a) (100); (b) (110); and (c) (111). The large circles represent top layer Ni atoms and the small circles represent the second layer. The surface unit cells are indicated by the real lines.

the (100) facet site (4) than that of the two (111) facet sites (3). We have also calculated the total energy of a C atom inside the cluster. The C atom is located at the interstitial site at the center of the cluster with a coordination number of six. The total energy is 1.20 eV higher than that of the (100) facet adsorption site after a full relaxation. This indicates that a C atom prefers to stay on the surface of the cluster.

The geometry of a clean Ni surface is optimized for each of the three, extended low-index surfaces, i.e., the (100), (110), and (111) surfaces, prior to adsorption of the C atom. Except for the contraction of the layer spacing, there is no surface reconstruction observed for all of the three surfaces, in agreement with the previous first-principles calculations of these surfaces.⁵⁴ After C adsorption, each slab is subsequently relaxed to reach the minimum-energy configuration.

The most stable adsorption site for the (100) surface is found at the highly symmetric hollow site, as shown in Fig. 3(a). There is no substantial relaxation of the surrounding Ni atoms after the adsorption. The site has a coordination number of four Ni atoms. Since there is only one C atom in a (6 × 6) (100) supercell, the corresponding coverage is so low that the clock-like surface reconstruction observed at about 0.5 ML coverage on the Ni (100) surface^{27,55} is not a concern. The most stable adsorption site for the (110) surface is found at the symmetric hollow site, as shown in Fig. 3(b). The relaxation for the nearest-neighboring Ni atoms is substantial. These Ni atoms move toward the adsorbed C atom. The coordination number at this site is five since the distance from the bottom Ni atom on the second layer to the C atom is 1.92 Å, just 1% larger than the distance from the other four Ni atoms (~1.90 Å). There are two stable adsorption sites for the (111) surface. One is at the hcp site and another is at the fcc site, as indicated in Fig. 3(c). Both sites have a coordination number of three Ni atoms. The only difference between the two sites is the environment at the second Ni layer. The energies at the two sites are within several hundredths of eV, comparable to the accuracy of our calculations, which we estimated as ~0.03 eV. In the test of the slabs with double thickness, which is mentioned at the end of Sec. III, the order of the two were reversed, but still within several hundredths of eV. So we note that our model is not accurate enough to determine their sequence. The relaxation of the Ni atoms at both sites upon C adsorption is minor.

The binding energies E_b , which is defined as $E_b = E_{\text{tot}}(\text{Ni-slab}) + E_{\text{tot}}(\text{C atom}) - E_{\text{tot}}(\text{C/Ni-slab})$ where E_{tot} is the total energy of the system indicated in the parenthesis, is obtained for each adsorption configuration. They are listed in Table II. The highest binding energy occurs at the (100) site, which is 8.43 eV, surprisingly close to the value (8.26 eV) for the (100) facet of the Ni₃₈ cluster. Meanwhile, the (110) surface site and the hcp and fcc sites on the (111) surface have the lower binding energies in descending order. Compared with the Ni₃₈ cluster results, apart from the lack of the (110) facet in Ni₃₈, the energetics of the sites for C atom adsorption on both the Ni₃₈ cluster and the extended Ni surfaces have exactly the same order. On the other hand, the available C–Ni bond lengths for both Ni₃₈ and the extended surfaces are consistent, which agree well with the existing experiments (see Table II). Considering the huge difference in the curvature of the two extreme cases, this is a remarkable result. We could assume that this preference order and the values of E_b 's for the adsorptions of a C atom on any Ni cluster with a curvature between them will be preserved. By examining the coordination numbers of Ni atoms and the bond lengths for the surface adsorption, there is a correlation between them, a higher coordination number leads to a longer bond length. Similar to the cluster case, the coordination of four is preferred by the adsorbed C atom.

The Ni₃₈ cluster is only a model system chosen for the cluster case of small size and hence large curvature. On the other hand, the extended low-index surfaces are the extreme case for clusters with much larger sizes. But both systems show that the (100) site is favored by the C adsorption. The binding energy values are more or less the same, indicating

TABLE III. The diffusion barriers on the three low-index surfaces as indicated in Fig. 3 and discussed in the text.

Surface	(100)	(110) along the trough	(110) across the trough	(111)
Saddle point	bridge	M	short bridge	bridge
Barrier height (eV)	2.19	0.60	1.46	0.37

the dominance of nearest neighbors of the adsorption site on this issue. This agrees with recent experimental results for binding energies of C atoms to nickel cluster cations which show convergence of binding energies (within ± 0.5 eV) to about 6.5 eV for cluster sizes greater than $n = 5$.¹⁵ This behavior may be understood in terms of simple bond ordering and atom coordination arguments.^{12,16} The interaction between C and Ni atoms is short-ranged since we believe that electrons from the carbon atom would be filled predominantly in nickel's partially occupied d -bands/orbitals, which are localized in space. So the interaction with the nearest-neighbor Ni atoms play dominant roles.

The mobility of an adsorbed C atom on the various surfaces is a key fact to determine the nucleation, and hence the growth mechanism. The diffusion paths and the corresponding barriers of a C atom on the three low-index Ni surfaces are therefore studied. By symmetry consideration on each surface, we can assume the diffusion is just simply a hopping between the minima, and the saddle points are most likely at the bridges dividing any two neighboring adsorption sites (minima). The only exception is the diffusion path along the trough in the (110) surface. The nudge elastic band method⁵⁶ has been used to find the saddle points and diffusion barriers. They are listed in Table III. The saddle point of the diffusion path for the (100) surface is at the bridge between the two neighboring hollow sites, with an energy barrier of 2.19 eV. Due to the lower symmetry of the (110) surface, there are two available diffusion paths. One is along the trough while another is across the trough [see Fig. 3(b)]. The saddle point for the path across the trough is at the short-bridge with a barrier of 1.46 eV. The saddle point for the diffusion along the trough is at the middle between the hollow site and the long bridge [see Fig. 3(b)] with a barrier of 0.60 eV. The long bridge site turns out to be a local minimum, just 0.16 eV higher energetically than the hollow site. The diffusion path on the (111) surface is determined along the connection of an fcc site to its nearby hcp site, with a 0.37 eV barrier at the bridge. By comparison, the diffusion on the Ni(111) surface has overall the lowest barrier.

V. CONCLUSION

The present study provides insight into the adsorption and diffusion for a single C atom on Ni surfaces. The result will provide us useful information to understand the initial stage of the nucleation for SWNTs. It is still far from a complete picture for the nucleation and growth.

In conclusion, we have studied the adsorption of a carbon atom on the Ni₃₈ cluster and the three low-index Ni surfaces, namely (100), (110), and (111), by DFT calculations with the GGA treatment to the exchange-correlation functional. The binding energies of a C atom on the low-index Ni surfaces and the corresponding facets on the Ni₃₈ cluster have been obtained and compared. Both the binding energies and the bond lengths have a good agreement with experiment. The (100) hollow site is favored by C atom adsorption. In spite of the huge difference in the curvature, the preference order of the sites for the C atom is unchanged. This preference order is expected to be kept in large Ni clusters, to which a DFT calculation is not feasible currently. A coordination number of 4 for C on the surface is always preferred. Although the (100) surface is favored for C adsorption, the mobility may restrict it from being favored by nucleation for carbon tube growth. The (111) surface has the lowest diffusion barrier and hence the highest mobility for the C atom.

ACKNOWLEDGMENTS

We are grateful to R. F. Wood for beneficial discussions. This work was partially supported by the Laboratory Directed Research and Development Program of Oak Ridge National Laboratory (ORNL), managed by UT-Battelle, LLC for the U. S. Department of Energy under Contract No. DE-AC05-00OR22725, and National Natural Science Foundation (NNSF) of China. The computations were done at National Energy Research Scientific Computing Center (NERSC) of the DOE, the high-performance computing center in the University of Texas at Arlington, and the Center for Computational Sciences (CCS) at ORNL.

¹For review, see R. T. K. Baker and P. S. Harris, in *Chemistry and Physics of Carbon*, edited by P. L. Walker *et al.* (Dekker, New York, 1978), Vol. 14, p. 83.

²C. Journet, W. K. Maser, P. Bernier, A. Loiseau, M. Lamy de la Chapelle, S. Lefrant, P. Deniard, R. Lee, and J. E. Fischer, *Nature* (London) **388**, 756 (1997).

³A. Thess, R. Lee, P. Nikolaev, H. Dai, P. Petit, J. Robert, C. Xu,

Y. H. Lee, S. G. Kim, A. G. Rinzler, D. T. Colbert, G. E. Scuseria, D. Tománek, J. E. Fischer, and R. E. Smalley, *Science* **273**, 483 (1996).

⁴S. Bandow, S. Asaka, Y. Saito, A. M. Rao, L. Grigorian, E. Richter, and P. C. Eklund, *Phys. Rev. Lett.* **80**, 3779 (1998).

⁵D. Laplaze, P. Bernier, W. K. Maser, G. Flamant, T. Guillard, and A. Loiseau, *Carbon* **36**, 685 (1998).

- ⁶H. Dai, A. G. Rinzler, P. Nikolaev, A. Thess, D. T. Colbert, and R. E. Smalley, *Chem. Phys. Lett.* **260**, 471 (1996).
- ⁷H. M. Cheng, F. Li, G. Su, H. Y. Pan, L. L. He, X. Sun, and M. S. Dresselhaus, *Appl. Phys. Lett.* **72**, 3282 (1998).
- ⁸P. Nikolaev, M. J. Bronikowski, R. K. Bradley, F. Rohmund, D. T. Colbert, K. A. Smith, and R. E. Smalley, *Chem. Phys. Lett.* **313**, 91 (1999); M. J. Bronikowski, P. A. Willis, D. T. Colbert, K. A. Smith, and R. E. Smalley, *J. Vac. Sci. Technol. A* **19**, 1800 (2001).
- ⁹J. W. Gadzuk, in *Surface Physics of Materials*, edited by J. M. Blakely (Academic, New York, 1975); J. B. Benziger, in *Metal-Surface Reaction Energetics*, edited by E. Shustorovich (VCH, New York, 1991); A. Ya. Tontegode, *Prog. Surf. Sci.* **38**, 201 (1991).
- ¹⁰J. Shelton, H. Patil, and J. Blakely, *Surf. Sci.* **43**, 493 (1974).
- ¹¹L. C. Isett and J. M. Blakely, *Surf. Sci.* **47**, 645 (1975).
- ¹²L. C. Isett and J. M. Blakely, *Surf. Sci.* **58**, 397 (1976).
- ¹³M. Eizenberg and J. Blakely, *Surf. Sci.* **82**, 228 (1979).
- ¹⁴A. Takeuchi and H. Wise, *J. Phys. Chem.* **87**, 5372 (1983).
- ¹⁵F. Liu and P. B. Armentrout (private communication).
- ¹⁶R. Liyanage, X.-G. Zhang, and P. B. Armentrout, *J. Chem. Phys.* **115**, 9747 (2001).
- ¹⁷K. W. Jacobsen and J. K. Norskov, *Surf. Sci.* **166**, 539 (1986).
- ¹⁸G. R. Darling, J. B. Pendry, and R. W. Joyner, *Surf. Sci.* **221**, 69 (1989).
- ¹⁹K. W. Frese, Jr., *Surf. Sci.* **182**, 85 (1987).
- ²⁰A. D. van Langeveld, A. de Koster, and R. A. van Santen, *Surf. Sci.* **225**, 143 (1990).
- ²¹A. de Koster and R. A. van Santen, *J. Catal.* **127**, 141 (1991).
- ²²W.-X. Zhang, Q.-A. Qiao, S.-G. Chen, M. C. Cai, and Z. X. Wang, *Chin. J. Chem.* **19**, 325 (2001).
- ²³J. K. Onuferko, D. P. Woodruff, and B. W. Holland, *Surf. Sci.* **87**, 357 (1979).
- ²⁴M. Bader, C. Ocal, B. Hilbert, J. Hasse, and A. M. Bradshaw, *Phys. Rev. B* **35**, 5900 (1987).
- ²⁵D. Arivaanitis, K. Baberschke, and L. Wenzel, *Phys. Rev. B* **37**, 7143 (1988).
- ²⁶A. L. D. Kilcoyoe, D. P. Woodruff, A. Robison, T. Linder, J. S. Somers, and A. M. Bradshaw, *Surf. Sci.* **253**, 107 (1991).
- ²⁷R. Terborg, J. T. Hoeft, M. Polcik, R. Lindsay, O. Schaff, A. M. Bradshaw, R. L. Toomes, N. A. Booth, D. P. Woodruff, E. Rotenberg, and J. Denlinger, *Surf. Sci.* **446**, 301 (2000).
- ²⁸S. Takatoh, K. Arai, T. Hayashi, T. Enokijima, T. Yikegaki, J. Tsukajima, T. Fujikawa, and S. Usami, *Physica B* **208&209**, 245 (1995).
- ²⁹*The Challenge of d and f Electrons: Theory and Computation*, edited by D. R. Salahub and M. C. Zerner (American Chemical Society, Washington, D.C., 1989).
- ³⁰J. A. Alonzo, *Chem. Rev. (Washington, D.C.)* **100**, 637 (2000).
- ³¹J. E. Müller, M. Wuttig, and H. Ibach, *Phys. Rev. Lett.* **56**, 1583 (1986).
- ³²I. Panas, J. Schüle, U. Brandemark, P. Seigbahn, and U. Wahlgren, *J. Phys. Chem.* **92**, 3079 (1988).
- ³³R. Fournier, J. Andzelm, A. Goursot, N. Russo, and D. R. Salahub, *J. Chem. Phys.* **93**, 2919 (1990).
- ³⁴H. Burghgraef, A. P. J. Jansen, and R. A. van Santen, *Surf. Sci.* **324**, 345 (1995).
- ³⁵G. S. Painter and F. W. Averill, *Phys. Rev. B* **26**, 1781 (1982).
- ³⁶A. D. Becke, *Int. J. Quantum Chem.* **27**, 5048 (1981).
- ³⁷J. C. Grossman, L. Mitas, and K. Raghavachari, *Phys. Rev. Lett.* **75**, 3870 (1995).
- ³⁸L. Mitas, J. C. Grossman, I. Stich, and J. Tobik, *Phys. Rev. Lett.* **84**, 1479 (2000).
- ³⁹D. J. Klink II, S. Wilke, and L. J. Broadbelt, *J. Catal.* **178**, 540 (1998).
- ⁴⁰R. M. Watwe, H. S. Bengaard, J. R. Rostrup-Nielsen, J. A. Dumesic, and J. K. Norskov, *J. Catal.* **189**, 16 (2000).
- ⁴¹G. Kresse and J. Furthmüller, *Comput. Mater. Sci.* **6**, 15 (1996); *Phys. Rev. B* **54**, 11 169 (1996).
- ⁴²J. P. Perdew, J. A. Chevary, S. H. Vosko, K. A. Jackson, D. J. Sign, and C. Fiolhais, *Phys. Rev. B* **46**, 6671 (1992).
- ⁴³M. C. Vargas, P. Giannozzi, A. Selloni, and G. Scoles, *J. Phys. Chem. B* **105**, 9505 (2001), and references therein.
- ⁴⁴D. Vanderbilt, *Phys. Rev. B* **41**, 7892 (1990).
- ⁴⁵E. G. Moroni, G. Kresse, J. Hafner, and J. Furthmüller, *Phys. Rev. B* **56**, 15 629 (1997).
- ⁴⁶B. V. Reddy, S. K. Nayak, S. N. Khanna, B. K. Rao, and P. Jena, *J. Phys. Chem. A* **102**, 1748 (1998).
- ⁴⁷A. A. Radzig and B. M. Smirnov, *Reference Data on Atoms, Molecules, and Ions* (Springer-Verlag, Berlin, 1985).
- ⁴⁸M. D. Morse, G. P. Hansen, P. R. R. Langridge-Smith, Lan-Sun Zheng, M. E. Geusic, D. L. Michalopoulos, and R. E. Smalley, *J. Chem. Phys.* **80**, 5400 (1984).
- ⁴⁹Since we use no-spin-polarized calculations, the ground state obtained for C and Ni is a singlet while the real ground state measured by experiments is a triplet. We have used the experimental ground triplet-singlet energy difference [C (Ref. 50) and Ni (Ref. 51)] to correct our atomic ground state when we calculate the binding energies, and later on the binding energies.
- ⁵⁰C. E. Moore, in *CRC Handbook of Chemistry and Physics*, 76th ed., edited by J. W. Gallagher (CRC Press, Boca Raton, FL, 1993), p. 336.
- ⁵¹J. Sugar and C. Corliss, *J. Phys. Chem. Ref. Data, Suppl.* **2** **14**, 581 (1985).
- ⁵²Y. Xiang, D. Y. Sun, and X. G. Gong, *J. Phys. Chem. A* **104**, 2746 (2000).
- ⁵³E. K. Parks, G. C. Nieman, K. P. Kerns, and S. J. Riley, *J. Chem. Phys.* **107**, 1861 (1997).
- ⁵⁴G. Kresse and J. Hafner, *Surf. Sci.* **459**, 287 (2000).
- ⁵⁵J. H. Onuferko, D. P. Woodruff, and B. W. Holland, *Surf. Sci.* **87**, 357 (1979).
- ⁵⁶H. Jónsson, G. Mills, and K. W. Jacobsen, in *Classical and Quantum Dynamics in Condensed Phase Simulations*, edited by B. J. Berne, G. Ciccotti, and D. F. Coker (World Scientific, Singapore, 1998), p. 385.